Proximity Forces*

J. Błocki,[†] J. Randrup,[‡] W. J. Świątecki, and C. F. Tsang

Lawrence Berkeley Laboratory, University of California, Berkeley, California 94720

Received August 6, 1976

We have generalized a theorem according to which the force between two gently curved objects in close proximity is proportional to the interaction potential per unit area between two flat surfaces made of the same material, the constant of proportionality being a measure of the mean curvature of the two objects. This theorem leads to a formula for the interaction potential between curved objects (e.g., two smooth cylinders of mica or two atomic nuclei) which is a product of a simple geometrical factor and a universal function of separation, characteristic of the material of which the objects are made, and intimately related to the surface energy coefficient. We have calculated and tabulated this universal function for nuclear surfaces, using the nuclear Thomas–Fermi approximation. The results can be expressed by a simple cubic-exponential formula which gives the potential between any two nuclei in the separation degree of freedom. Even simpler expressions are found for the interaction energy associated with the "crevice" or neck in the nuclear configuration that would be expected immediately after contact of two nuclei. These "proximity energies" are used to supplement the usual expansion of the energy of a thin-skinned system into volume, surface, curvature, and higher-order terms. The resulting elementary formulas are tested against explicit models of interacting nuclei and against elastic scattering data, and are found to be useful for even quite small mass numbers.

1. INTRODUCTION

For certain physical systems such as homogeneous solids, fluids, or the heavier atomic nuclei, made up of elements interacting by short-range forces and possessing a surface region which is thin compared to the size of the object under consideration (leptodermous systems), the potential energy of the system may be decomposed into a bulk term and a surface-layer term. The surface-layer term is associated with the surface region and is, therefore, approximately proportional to the area of the surface bounding the object. For a simply-connected system the above decomposition is accurate if the principal radii of curvature of the surface are everywhere much larger than the thickness of the surface region. Moreover, when this condition is satisfied, corrections to the leading area-proportional term in the surface-layer energy (such as

427

the curvature correction) may be derived by expansions in powers of the ratio of the thickness of the surface to the size of the system, thus making the expression for the potential energy even more accurate (see Section 3). Such a series expansion has been useful in discussing the average binding energies (masses) of atomic nuclei, and one might have thought that, apart from effects associated with the discreteness of nucleons (shell effects) there was no more to the problem of average nuclear energies than the calculation of the above series expansions to a sufficiently high order. This is not the case. Thus, when the surface of the system becomes contorted into features whose characteristic dimensions are of the order of the thickness of the surface region itself, the above series expansions become of limited usefulness. This failing is by no means of merely academic interest; it is serious for a system with a thin neck, on the verge of dividing into two fragments (as in nuclear fission), or in the case of two subsystems about to come into contact (as in collisions between heavy nuclei). In the latter case in particular, when the system is not simply connected, a calculation of the surface-layer energies of the two pieces, no matter how accurately they are corrected for the curvatures of the two surfaces, can never give rise to the (strong) attraction that in practice appears when the two surfaces approach to within a distance comparable with the surface thickness.

Various attempts to remedy these failings have been made in the past. They range from microscopic computer calculations on individual pairs of nuclei [1-3] through various folding prescriptions where a potential well is folded into a density distribution [4-6], to direct estimates of certain aspects of the nucleus-nucleus force in terms of the experimentally known surface-energy coefficient [7,8].

In line with the latter developments we have found it possible to derive simple expressions for the additional potential energy (or forces) associated with certain of the more important types of violently contorted surfaces, which should enable one to complement in a useful way the usual series expansions of the nuclear energy. We shall call these additional forces "proximity forces" because they arise from the proximity of elements of the contorted surface, the contortion being such that different pieces of the surface actually face each other across a (small) gap or crevice. In particular we have rederived and extended a theorem that makes it possible to relate (approximately) the interaction between two finite nuclei to the interaction between two flat parallel slabs of semi-infinite nuclear matter, a problem that is simpler, and can be solved (in a suitable approximation) once and for all. (The derivation of the theorem, in many essential aspects, is contained in a 1934 paper by Deryagin [9] on coagulation of aerosols. We are grateful to H. J. Krappe for pointing this out to us.)

2. THE PROXIMITY ENERGY

The starting point of our considerations is an expression for the proximity energy V_p associated with a curved gap or crevice of gently variable width D, which we shall write in the form

$$V_P = \iint e(D) \, d\sigma + \text{corrections.} \tag{1}$$

Here $e(D)$ is the interaction energy per unit area of two *parallel* surfaces at the appropriate separation D. The integral is over the area of the gap or crevice and the "corrections" become negligible as the curvatures of the surfaces defining the gap become small.

The geometry of the gently variable gap may be specified by first choosing a mean gap surface Γ (a two-dimensional surface in space) and then considering normal displacements n_R, n_L, locating the right- and left-hand sides of the gap, $n_R - n_L = D(u, v)$ being the distance between the two sides Γ_L, Γ_R of the gap. The gap width $D(u, v)$ is a (slowly varying) function of position on the surface Γ, the position being specified by two coordinates u and v, say.

Since $e(D)$ is, by definition, a function of only one variable, D, rather than of the two position variables u and v, the surface integral in Eq. (1) may be converted, at once, into a one-dimensional integral. Thus imagine that a family of (closed) curves (or sets of curves) is constructed on the surface Γ corresponding to constant values of D. Denote by $J(D)dD$ the area of the surface Γ that lies between two such curves (or sets of curves) defined by D and $D + dD$. Then we may write

$$V_P = \int e(D) \, J(D) \, dD + \cdots . \tag{2}$$

The function $J(D)$ is characteristic of the geometry of the gap, and thus if the two sides of the gap are shifted, rotated, or deformed in some way so that the gap surface Γ and gap width D are changed, J will be a function (strictly speaking a functional) of these shifts, rotations, or deformations. We shall write $J(\alpha, D)$ to exhibit explicitly the dependence of J on the set of degrees of freedom α specifying the gap geometry. The function $e(D)$ (the interaction energy per unit area of two parallel surfaces) is, by definition, independent of the geometry of the gap. It does depend, however, on the nature of the surfaces. In particular, if the structure of the surface (e.g., the density falloff profile in the surface region) is considered as variable, and specified by a set of degrees of freedom β, we may exhibit this by writing $e(\beta, D)$. Thus our basic equation for the energy associated with a gently variable gap or crevice is

$$V_P(\alpha, \beta) = \int e(\beta, D) \, J(\alpha, D) \, dD + \cdots, \tag{3}$$

where α specifies the geometry of the gap and β specifies the structure of the surface region.

In what follows we shall specialize at once to the case of surfaces with an invariable structure corresponding to that of a standard plane surface at equilibrium, characterized by an equilibrium density profile and a standard surface-energy coefficient. (For a discussion of the dependence of e on the surface diffuseness see Refs. [10, 11].) As regards the geometry of the gap we shall illustrate the applications of Eq. (3) by several assumptions about the function $D(u, v)$ and the mean gap surface Γ.

2.1. *Gap with Gently Variable Paraboloidal Width*

Consider a mean gap surface Γ which is so gently curved that the coordinates u, v on the surface Γ may be taken as cartesian coordinates x, y, and the normal coordinate n used to specify the gap ($n_R - n_L = D$) may be taken as the cartesian coordinate z, with $z_R - z_L = D$. (Some attempts were made to derive the corrections arising from a finite curvature of Γ. However, the increase in the complexity of the formulas seemed to exceed in most cases the slight gain in accuracy obtained by working with a curved mean gap surface.) Consider now as an example a gap width $D(x, y)$ which has a least value $D = s$ at $x = y = 0$, say, and whose width in the vicinity of this point is given by the Taylor expansion

$$
\begin{aligned}
D(x, y) &= s + \tfrac{1}{2}D_{xx}x^2 + \tfrac{1}{2}D_{yy}y^2 + \cdots \\
&= s + \tfrac{1}{2}(x^2/R_x) + \tfrac{1}{2}(y^2/R_y) + \cdots .
\end{aligned}
\tag{4}
$$

In the above, D_{xx} and D_{yy} are the second derivatives of D with respect to x and y evaluated at the point of least gap width. In the second line these derivatives are written in terms of the principal radii of curvature, R_x and R_y, of the surface obtained by plotting the gap width D as a function of x and y. The directions of x and y are assumed to have been chosen along the principal axes of the quadratic form $D(x, y)$ so there is no cross term in xy in Eq. (4).

Now change variables from x, y to ξ, η, defined by $\xi = x/(2R_x)^{1/2}$, $\eta = y/(2R_y)^{1/2}$, so that D may be written as $D = s + \rho^2$, with $\rho^2 = \xi^2 + \eta^2$. The proximity energy can then be transformed as follows:

$$
V_P(s) = \iint dx \, dy \, e(D) \tag{5}
$$

$$
= 2(R_x R_y)^{1/2} \iint d\xi \, d\eta \, e(D)
$$

$$
= 2(R_x R_y)^{1/2} \int_0^{\infty} 2\pi\rho \, d\rho \, e(D)
$$

$$
= 2\pi\bar{R} \int_{D=s}^{\infty} dD \, e(D)
$$

$$
= 2\pi\bar{R}\mathscr{E}(s). \tag{6}
$$

In the last few lines the integration has been extended to infinity. This assumes that the gap width grows to *beyond the range of* the interaction function $e(D)$ and that $e(D)$ approaches zero sufficiently rapidly for large values of D so that the integral becomes essentially independent of the upper limit. (Note that this means that, with D given by Eq. (4), Eq. (6) is valid for any finite value of R_x^{-1}, R_y^{-1}, however small, but *not* for $R_x^{-1} = 0$, $R_y^{-1} = 0$, which would correspond to a *parallel* gap whose sides *never* get outside the range of $e(D)$.) The quantity $\bar{R}$ is the geometric mean of the two principal radii of curvature R_x, R_y, characterizing the gap D. The reciprocal of $\bar{R}$ is $1/(R_x R_y)^{1/2}$,

the square root of the invariant Gaussian curvature at $x = y = 0$ of the surface obtained by plotting D versus x and y.

The negative of the partial derivative of $V_P(s)$ with respect to s gives the force between the two surfaces as a function of the separation degree of freedom

$$F(s) = -(\partial V_P/\partial s) = 2\pi \bar{R} e(s). \tag{7}$$

This leads to the following Proximity Force Theorem

The force between two gently curved surfaces as a function of the separation degree of freedom s is proportional to the interaction potential per unit area, e(s), between two flat surfaces, the proportionality factor being 2π times the reciprocal of the square root of the Gaussian curvature of the gap width function at the point of closest approach.

In the case of two spherical surfaces with radii C_1 and C_2 the equation for D is

$$D = s + \tfrac{1}{2}((1/C_1) + (1/C_2)) x^2 + \tfrac{1}{2}((1/C_1 + (1/C_2)) y^2 + \cdots$$

so that the mean curvature radius $\bar{R}$ becomes $\bar{R} - C_1 C_2/(C_1 + C_2)$, a kind of "reduced radius" of the two spheres (like a reduced mass $M_1 M_2/(M_1 + M_2)$).

The usefulness of the Proximity Force Theorem lies in the circumstance that the principal features of the function $e(s)$ may be derived from experimentally known surface properties, such as the surface energy coefficient γ and the degree of diffuseness of the surface layer. Thus for s greater than the thickness of the surface (2 or 3 fermis in the case of nuclei) $e(s)$ tends rapidly to zero. For smaller values of s, $e(s)$ becomes negative, and for $s = 0$ it is approximately equal to minus twice the surface energy per unit area of the material of which the system is composed. This is because at $s = 0$ the two juxtaposed density distributions add up to an approximately constant bulk value, so that the net effect of bringing the surfaces together from infinity is to destroy the two surfaces. Thus $e(0) \approx -2\gamma$, where γ is the surface energy coefficient (about 1 MeV/fm² for nuclear matter, about 75 ergs/cm² for water).

If one were to continue on to negative values of s, adding up the two density distributions without allowing them to get out of each other's way, the function $e(s)$ would begin to increase, would go through zero, and would eventually grow without limit, reflecting the energy cost of doubling the density in the overlap region. It follows that $e(s)$ exhibits a minimum, and this minimum occurs in fact near $s = 0$, where $e(0) \approx -2\gamma$. This is because it is at this separation that the total density is approximately equal to the standard bulk density, and the bulk energy of stable saturating systems (such as nuclei or ordinary matter) is a minimum with respect to deviations of the density from the standard value. From this circumstance follows an interesting result. The *maximum* attraction predicted by Eq. (7) occurs where $e(s)$ is most negative, and this as we saw occurs at $s \approx 0$ where $e \approx -2\gamma$. Hence

$$\text{Maximum Attraction} \approx 2\pi \bar{R} e(0)$$
$$\approx -4\pi \bar{R} \gamma. \tag{8}$$

This equation expresses the remarkable result that the maximum attraction (in the separation degree of freedom) between gently curved bodies may be written down approximately without any knowledge of the nature of the cohesive interactions between the particles constituting the bodies, provided only the surface energy coefficient is known.

As the two curved objects begin to overlap beyond the point of maximum attraction at $s \approx 0$, the attraction in the separation degree of freedom decreases and becomes zero at some point s_1 where the function $e(s_1)$ is zero. Since the zero(s) of $e(s)$ are, in the nature of things, independent of the curvatures of the two objects, we deduce a second noteworthy result. The equilibrium point (a minimum) in the separation degree of freedom for two gently curved objects, such as two (uncharged) nuclei, occurs at one and the same overlap distance s_1 for all pairs of nuclei, independently of their sizes. (Note, however, that infinitely large objects, two really flat surfaces, are, once again, an exception.)

Under the conditions stated Eq. (8) would apply equally well to the contact force in the separation degree of freedom between ordinary solids (where the attraction is due to molecular forces), or to nuclei, where the attraction is due to nucleon–nucleon forces. The magnitude of the force predicted by Eq. (8) may be illustrated as follows. With a nominal value of γ equal to 100 ergs/cm² (the surface energy of solids is of this order of magnitude, for example, 300 ergs/cm² for mica) we find that two equal spheres with radii 5 cm should attract each other with a force

$$F_{\max} = -3100 \text{ dyn} = -3.2 \text{ g weight.}$$

Cohesive forces between smooth curved surfaces of mica, rubber and gelatin have in fact been found experimentally to have this order of magnitude [12, 13].

In the case of nuclei the surface energy coefficient γ is about 1 Mev/fm² and for two equal spheres with radii 5 fm (corresponding approximately to medium nuclei with mass number 76) we find

$$F_{\max} \approx -31 \text{ MeV/fm} \approx -500 \text{ kg weight.}$$

In order to calculate the force between two nuclei in its dependence on the separation s one has to use Eq. (7), whose right-hand side is a product of a geometrical factor $2\pi \overline{R}$ depending on the two nuclei in question, and a *universal function of distance* $e(s)$, independent of the nuclei. The semiquantitative appearance of $e(s)$ has been sketched out above, but in order to calculate $e(s)$ in detail one needs to have a theory describing the structure of the nuclear surface region, so that one may take two flat nuclear surfaces and calculate their interaction energy per unit area as a function of the separation. We have performed such a calculation of $e(s)$ using a theory of the nuclear surface based on the Thomas–Fermi treatment. The results will be described in Section 4.

2.2 *Other Gap or Crevice Geometries*

The proximity potential may be readily generalized to other equations besides the paraboloidal relation between D and x, y given by Eq. (4).

First note that Eq. (5) for the proximity potential is invariant with respect to an area-preserving stretching and compression of the transverse coordinates from x, y to x', y' where $x' = \alpha x$, $y' = (1/\alpha)y$. It follows that even if we specialize to systems for which D is assumed to be only a function of the transverse radial distance r, where $r^2 = x^2 + y^2$, the results will hold, without any modifications, for "stretched" systems obtained by deforming the original circular contours of constant D into area-preserving ellipses. Conversely, in any problem where the contours of constant D are ellipses, the analysis may be simplified at once by considering the case of circular contours, where D is a function of r^2 only.

Consider now the relation between r^2 and D to be of the form

$$r^2 = \sum_{n=0}^{N} c_n D^n, \tag{9}$$

where c_n are arbitrary coefficients. Inserting Eq. (9) in Eq. (5) we find

$$V_P = \int 2\pi r \, dr \, e(D)$$

$$= \pi \sum_{1}^{N} n c_n \mathscr{E}_{n-1},$$

where the quantities

$$\mathscr{E}_n = \int_{s \text{ or } 0}^{\infty} D^n e(D) \, dD, \tag{10}$$

are moments of the universal function $e(D)$. The lower limit "s or 0" distinguishes between what we shall call a "gap" and a "crevice." The former means that D has a least value (say s) at $r = 0$. (This value may be negative, corresponding to an overlapping of the two bodies which, for large negative s, would lead to a region of doubled density.) The latter means that D becomes zero at some finite value of r, say a neck or crevice radius r_{neck} (related to c_0 by $r_{\text{neck}}^2 = c_0$), and there is no overlap or density doubling. Thus a gap refers to two bodies (overlapping or not) and a crevice to a single indented body.

The upper limit in Eq. (10) has been set equal to infinity under the same assumptions as before.

The case $N = 1$, with $c_1 = 2\bar{R}$ and $c_0 = -sc_1$ corresponds to the paraboloidal gap considered before. For a paraboloidal crevice (a crevice formed by portions of two intersecting paraboloids) we have

$$V_P = 2\pi\bar{R} \int_0^{\infty} e(D) \, dD.$$

Note that the proximity potential for a paraboloidal crevice with given $\bar{R}$ is independent of c_0 (or r_{neck}), i.e., is a constant independent of the degree of overlap.

It follows that the proximity potential along a sequence of configurations which for $s > 0$ consists of approaching gently curved surfaces (approximated by paraboloids) and for $s < 0$ turns into the corresponding crevice, exhibits a discontinuity in the first derivative at $s = 0$. This is because as s tends to zero from above, $\partial V_P/\partial s$ tends to about $4\pi\bar{R}\gamma$ (Eq. 8), whereas for $s < 0$, $\partial V_P/\partial s = 0$. As is readily verified, this $4\pi\bar{R}\gamma$ is precisely the negative of the discontinuity in the derivative of the *surface energy* that occurs when two gently curved surfaces characterized by a gap width curvature radius $\bar{R}$ turn into a crevice at contact. It follows that the addition of the proximity energy rounds off (approximately) the familiar kink that is present when only the surface energy is retained in the calculation of the potential for two fusing nuclei parametrized by separated or overlapping figures such as spheres or spheroids.

The case $N = 2$ corresponds to a relation between r^2 and D which defines a conic

$$r^2 = c_0 + c_1 D + c_2 D^2, \tag{11}$$

leading to

$$V_P = \pi c_1 \mathcal{E}_0 + 2\pi c_2 \mathcal{E}_1. \tag{12}$$

For gaps, $\mathcal{E}_0$ (the same as $\mathcal{E}$) and $\mathcal{E}_1$ are two universal functions of s, and for crevices two universal constants, characteristic of the material of which the surface is made.

Gaps or crevices corresponding to the following geometrical arrangements are covered by Eqs. (11), (12). (For crevices the overlapping portions are erased.)

(i) Two equal coaxial spheroids with semiaxes C, B (C along the line of centers) and tip distance s (which may be negative). The equation for D is in this case

$$(C + \tfrac{1}{2}s - \tfrac{1}{2}D)^2/C^2 + (r^2/B^2) = 1.$$

This is of the form of Eq. (11), with $c_1 = B^2(C + \tfrac{1}{2}s)/C^2$, $c_2 = -B^2/4C^2$. For two spheres $C = B$.

(ii) As above, but with one spheroid infinitely large (i.e., a plane). Thus we have a spheroid at a distance s from a plane, or a protuberance on a plane in the form of a portion of a spheroid. One readily verifies that in this case $c_1 = 2B^2(C + s)/C^2$, $c_2 = -B^2/C^2$. (In the general case of unequal spheroids N is infinite.)

(iii) For two equal juxtaposed hyperboloids with axes C, B (C along the line of centers) and tip distance s we find $c_1 = B^2(C - \tfrac{1}{2}s)/C^2$, $c_2 = B^2/4C^2$.

(iv) As above, but with one hyperboloid infinitely large (a plane) we find $c_1 = 2B^2(C - s)/C^2$, $C_2 = B^2/C^2$.

(v) For the case of a body in the form of a single hyperboloid of one or two sheets we have $c_1 = 0$, $c_2 = B^2/4C^2$. When the hyperboloid is of two sheets this is a special case of (iii). When the hyperboloid is of one sheet we have the case of a hyper-

boloidal crevice, a form often used to describe the neck shape of a fissioning nucleus or the crevice formed after contact of two nuclei.

(vi) For two juxtaposed coaxial circular cones with semiopening angles α_1 and α_2 and tip distance s (which as usual may be negative) we readily find $c_2 = (\cot \alpha_1 + \cot \alpha_2)^{-2}$, $c_1 = -2c_2 s$.

(vii) In addition, for the case of a gap between two coaxial elliptic paraboloids with tip distance s, with radii of curvature A_1 and B_1 in the principal planes of curvature through the tip of paraboloid 1, and A_2, B_2 for paraboloid 2, and an azimuthal angle ϕ between the principal planes of curvature of 1 and 2, we find $c_1 = 2\bar{R}$, $c_2 = 0$, where

$$\frac{1}{\bar{R}^2} = \frac{1}{A_1 B_1} + \frac{1}{A_2 B_2} + \left(\frac{1}{A_1 A_2} + \frac{1}{B_1 B_2}\right) \sin^2 \phi + \left(\frac{1}{A_1 B_2} + \frac{1}{A_2 B_1}\right) \cos^2 \phi.$$

This formula could be useful for discussing the nuclear force between two non-spherical nuclei. In this case, in addition to an attraction along the line of least separation, there is a torque around it, trying to align the principal planes of curvature in the vicinity of the point of least separation.

Note that the above results are valid insofar as the juxtaposed surfaces are nearly parallel. Contributions from parts of the surfaces where this is not satisfied cannot be expected to be given accurately. Fortunately these contributions usually tend to zero, which is at least qualitatively correct in most cases.

3. The Energy of Leptodermous Systems

In this section we shall give a derivation of the functional form of the energy of a leptodermous (thin-skinned) system in order to arrive at a total energy expression, including the proximity energy, which may be used as an approximation to the energy of many complicated systems in a variety of configurations of practical interest.

Consider a system with a particle density $\rho(\mathbf{r})$ and an energy density $\eta(\mathbf{r})$. The total number of particles is

$$A = \int \rho,$$

and the total energy is

$$E = \int \eta.$$

The integrals are over all space.

Note that no classical assumptions are made in defining ρ and η. For example, if the wave function of a system of A identical particles is $\psi(\mathbf{r}_1 \cdots \mathbf{r}_A)$ then the density ρ

and an energy density η may be defined in terms of the expectation values of the density and energy–density operators, leading to

$$\rho(\mathbf{r}_1) = A \int_{r_2} \cdots \int_{r_A} \psi^* \psi,$$

$$\eta(\mathbf{r}_1) = \int_{r_2} \cdots \int_{r_A} \psi^* H \psi,$$

where H is the Hamiltonian of the A-particle system.

In order to define a leptodermous system pick any number a_1 with the dimensions of an energy and form the identity

$$E = A a_1 + \int (\eta - a_1 \rho).$$

The definition of a leptodermous system is now as follows. If it is possible to find an a_1 such that the integrand $\eta - a_1 \rho$ is confined to a small neighborhood of a surface in space, then the system is leptodermous. "Small" means small compared to typical dimensions of the system.

As an example of a leptodermous system consider one with a density which looks like Fig. 1a, and an energy density η which looks like Fig. 1b. Now, if for a_1 we pick
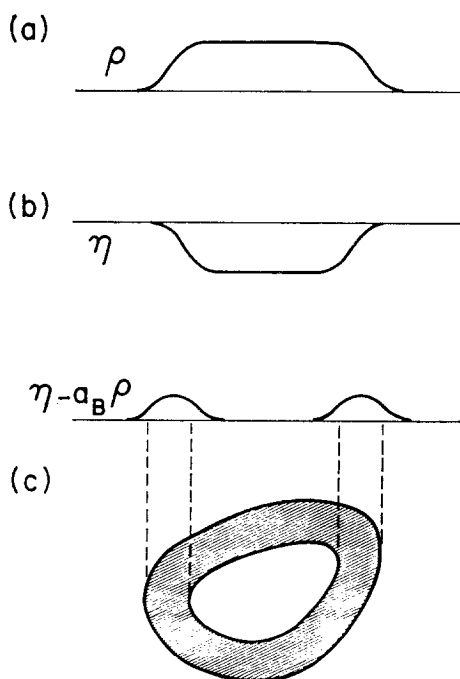

FIG. 1. A schematic illustration of the density ρ, energy density η, and surface-energy density function $\eta - a_B \rho$ for a leptodermous system.

the value of η/ρ in the bulk, say $a_B = \eta_B/\rho_B$, then $\eta - a_B\rho$ looks like Fig. 1c. The condition for the system to be leptodermous is that the bump in the integrand $\eta - a_B\rho$ should be localized near the surface, and in the case illustrated this is ensured because of the vanishing of η and ρ outside the system and the cancellation of η and $a_B\rho$ inside.

For some given physical system (a drop of water, a soap bubble, a degenerate Fermi gas in a container, an atomic nucleus, a hypothetical superdense nucleus [14], a "bag" or "bubble" model of a nucleon [15]) the answer to the question whether the leptodermous condition is satisfied or not may be sometimes obvious and sometimes subtle. It involves the examination of the energy–density bump function $\eta - a_1\rho$, in particular as regards the convergence of certain space integrals over this function. The discussion of this problem for various systems is outside the scope of this section, which will concern itself with the proof of the central theorem that follows if the leptodermous condition *is* satisfied.

THEOREM. *For a leptodermous system an approximation to the energy may be written* as

$$E = E_{\text{Bulk}} + E_{\text{Surface Layer}},\tag{13}$$

where

$$E_{\text{Bulk}} = a_B A$$
$$= c_1 \mathcal{V},$$

and

$$E_{\text{Surface Layer}} = c_2 \mathcal{S} + c_3 \mathcal{K} + c_4 \mathcal{G} + c_4' \mathcal{Q}$$
$$+ \text{ corrections that vanish as } A \to \infty + V_P.\tag{14}$$

In the above c_1, equal to η_B, is the energy per unit volume in the bulk, and $\mathcal{V}$ is the volume of the system *defined* by A/ρ_B. All the coefficients c_1, c_2, c_3, c_4, and c_4' are, in general, functions of the bulk density ρ_B, but are independent of the shape or size of the system. The shape and size dependence of the surface-layer energy for a fixed ρ_B is given by the following four functionals and by the proximity energy V_P

$$\mathcal{S} = \oint d\sigma = \text{ surface area,}$$

$$\mathcal{K} = \oint \kappa \, d\sigma = \text{ integrated curvature,}$$

$$\mathcal{G} = \oint \Gamma \, d\sigma = \text{ integrated Gaussian curvature,}\tag{15}$$

$$\mathcal{Q} = \oint \kappa^2 \, d\sigma = \text{ integrated squared curvature,}$$

$$V_P \approx \iint_{\text{gaps and crevices}} e(D) \, d\sigma.$$

Here the integrals $\oint$ are over the surface of the system, κ is the total curvature, and Γ the Gaussian curvature at a point on the surface

$$\kappa = (1/R_x) + (1/R_y),$$
$$\Gamma = (1/R_x R_y),$$

where R_x and R_y are the two principal radii of curvature at the point in question. The five terms c_1 to c_4' are the result of a systematic expansion of the energy in powers of the ratio of the surface thickness to the size of the system (the suffix indicates the relative order of the term). The underlying assumption is that the conditions in the vicinity of a point on the surface are functions only of the properties of the surface in the immediate neighborhood of that point. The proximity energy is an additional contribution that arises when the surface is so contorted that the conditions at some points are also functions of the location of a second nearly parallel piece of the surface brought into close proximity by the contortion of the surface.

To prove Eqs. (13), (14) consider first a plane surface region so that loci of constant density and constant energy density are plane parallel surfaces. The surface energy function $\eta - a_B\rho$ is, by hypothesis, effectively confined to a limited region, of width of the order of b, say (a length). Integrating $\eta - a_B\rho$ in the direction normal to the surface inside a "normal tube" of unit cross section gives the standard surface energy coefficient, which we shall denote by γ_0. (The integral over η is the actual energy, the integral over $a_B\rho$ is the energy that the same amount of matter would have if it were in the bulk, and so the difference is the surface energy.)

Imagine now the surface to be gently curved so that the surfaces of constant ρ are curved and the normals to these surfaces can be used to construct slightly curved normal tubes with somewhat variable cross sections. Define now an effective sharp surface Σ of the density distribution as that surface which cuts off a given infinitesimal tube at just such a point that as much material is in the tube outside the cut as would be needed to make up the density inside the cut to a uniform bulk value. The surface layer energy may then be written as

$$E_{SL} = \iiint (\eta - a_B\rho) = \iint_\Sigma d\sigma\,\gamma, \tag{16}$$

where the double integral is over the surface Σ, and $d\sigma\gamma$ stands for the result of integrating $\eta - a_B\rho$ inside a tube that intercepts the surface Σ in the infinitesimal area element $d\sigma$. The local surface energy coefficient γ thus defined may now vary from point to point on the surface Σ. We shall at first assume that it can be only a function of the *local* properties of the surface Σ at a given point. These local properties of Σ are the various curvature, inflection, and higher-order invariants of the surface at a given point, as revealed by a Taylor expansion of the surface in the vicinity of that point. Consider then the equation for the surface Σ in the vicinity of a point P to be written in cartesian coordinates as

$$z(x, y) = \tfrac{1}{2}z_{xx}x^2 + \tfrac{1}{2}z_{yy}y^2 + \tfrac{1}{6}z_{xxx}x^3 + \tfrac{1}{2}z_{xxy}x^2 y$$
$$+ \tfrac{1}{2}z_{xyy}xy^2 + \tfrac{1}{6}z_{yyy}y^3 + \cdots. \tag{17}$$

The origin of the coordinates has been chosen at P with the z-coordinate along the normal and the x–y coordinates in the tangent plane at P. (The orientation of the x–y axes has been chosen so that the cross term in xy does not appear in Eq. (17).) The symbols z_{xx}, z_{xxy}, etc., stand for the repeated derivatives of $z(x, y)$ with respect to x and y, evaluated at P. The second derivatives have the dimension (length)$^{-1}$ (they are the reciprocals of the principal radii of curvature R_x, R_y at P). The third derivatives have the dimension (length)$^{-2}$, and so on. Except for violently contorted regions of the surface these lengths may be taken to be not less in order of magnitude than a typical dimension of the shape in question, such as the radius R_0 of the equivalent sphere of equal volume. The *dimensionless* quantities of which the local surface energy γ can be a function are thus bz_{xx}, bz_{yy}, $b^2 z_{xxx}$, $b^2 z_{xxy}$, etc., which are of order b/R_0, $(b/R_0)^2$, etc. Thus we have

$$\gamma = \gamma(bz_{xx}, bz_{yy}, b^2 z_{xxx}, b^2 z_{xxy}, b^2 z_{xyy}, b^2 z_{yyy}, \cdots).$$

For a gently curved surface the dimensionless arguments are all small and we may in turn expand γ in a Taylor series

$$\gamma = \gamma_0 + k_1 b z_{xx} + k_2 b z_{yy} + k_3 b^2 z_{xx}^2 + k_4 b^2 z_{yy}^2 + k_5 b^2 z_{xx} z_{yy}$$

$$+ k_6 b^2 z_{xxx} + k_7 b^2 z_{xxy} + k_8 b^2 z_{xyy} + k_9 b^2 z_{yyy} + \text{ higher powers of } b. \quad (18)$$

Here γ_0 is the surface energy per unit area of a plane surface and $k_1 \cdots k_9$ are expansion coefficients. For example, $k_6 b^2$ is the derivative of the surface energy coefficient γ with respect to a cubic type of bending of the surface described by the term $\frac{1}{6} z_{xxx} x^3$ in Eq. (17), the derivative (with respect to $b^2 z_{xxx}$) being evaluated for $z_{xxx} = 0$, i.e., for a plane surface. Thus k_6 describes the *response* of a plane surface to an x^3 type of bending. From this it follows at once that all the coefficients k_6 to k_9 (those multiplying odd derivatives of z) must be zero. This is because the response of a plane surface to a bending associated with z_{xxx}, say, must be identical to the response associated with *minus* z_{xxx}, the two bent surfaces differing from one another only by a reflection in one of the coordinate planes. (The $x = 0$ plane in this case.) Thus γ must be an *even* function of the *odd* derivatives, and so must not contain linear terms in z_{xxx}, z_{xxy}, etc. It is also clear that k_1 must be equal to k_2, and k_3 must be equal to k_4 (the response of a plane to bendings in any two directions, such as x and y, must be identically the same.). It follows that γ may be written simply as

$$\gamma = \gamma_0 + K_1 \left(\frac{1}{R_x} + \frac{1}{R_y} \right) + K_3 \left(\frac{1}{R_x^2} + \frac{1}{R_y^2} \right) + K_5 \frac{1}{R_x R_y}$$

$$+ \text{ terms of order } (b/R_0)^3 \text{ and higher,}$$

$$= \gamma_0 + K_1 \kappa + K_3 \kappa^2 + (K_5 - 2K_3) \Gamma + \cdots,$$

where $\kappa = R_x^{-1} + R_y^{-1}$, $\Gamma = (R_x R_y)^{-1}$, and where the coefficients K are the following derivatives describing the response of a plane surface to infinitesimal bendings

$$K_1 = \left. \frac{\partial \gamma}{\partial \kappa} \right|_{\text{plane}} = \left. \frac{\partial \gamma}{\partial (R_x^{-1})} \right|_{\text{plane}},$$

$$K_3 = \left. \frac{1}{2} \frac{\partial^2 \gamma}{\partial (R_x^{-1})^2} \right|_{\text{plane}}, \qquad (19)$$

$$K_5 = \left. \frac{\partial^2 \gamma}{\partial (R_x^{-1}) \, \partial (R_y^{-1})} \right|_{\text{plane}}.$$

The total surface-layer energy of a gently curved leptodermous system is then

$$\begin{aligned}
E_{\text{SL}} &= \iint \gamma \, d\sigma \\
&= c_2 \mathscr{S} + c_3 \mathscr{K} + (c_4 \mathscr{G} + c_4' \mathscr{Q}) + \text{higher order terms},
\end{aligned} \qquad (20)$$

where $c_2 = \gamma_0$, $c_3 = K_1$, $c_4 = K_5 - 2K_3$, $c_4' = K_3$, and $\mathscr{S}, \mathscr{K}, \mathscr{G}, \mathscr{Q}$ are defined by Eqs. (15).

For a given bulk density ρ_B the coefficients $c_1 \cdots c_4'$ are constants and the total energy of the system is an expansion whose terms are readily verified to be of order $(R_0/b)^3$, $(R_0/b)^2$, (R_0/b), and $(R_0/b)^0$. Since, for a constant ρ_B, the radius R_0 is proportional to $A^{1/3}$, the terms are of order A, $A^{2/3}$, $A^{1/3}$, A^0, with corrections that tend to zero as A tends to ∞. An important point established in this section is thus that in order to discuss the energy of a gently curved leptodermous system even up to and including terms of order A^0, one does not need to calculate higher inflection invariants of the surface beyond the standard total and Gaussian curvatures κ and Γ, expressible in terms of the two elementary principal radii of curvature R_x and R_y.

The addition of the proximity energy V_P to the surface-layer energy (20) broadens the energy expression to include situations when the conditions at some points on a surface are no longer functions of only local properties, but depend on the presence of other juxtaposed, nearly parallel surface elements.

Of the three curvature correction functionals $\mathscr{K}, \mathscr{G}, \mathscr{Q}$, the integrated Gaussian curvature $\mathscr{G}$ is equal to 2π times the Euler–Poincaré characteristic χ of a surface (e.g., Ref. [32]). This quantity is characteristic of the topology of a surface but otherwise independent of its shape. (To determine χ for a given surface, subdivide the surface into a set of simple polygonal faces by drawing a set of edges coming together at a set of vertices. The number of vertices, minus the number of edges, plus the number of faces, gives χ.) Thus $\mathscr{G}$ is 4π for surfaces with the topology of a single fragment, $4\pi n$ for n fragments, zero for a torus or bubble nucleus, etc. The inclusion of $\mathscr{G}$ in the leptodermous series for arbitrary shapes is thus a trivial matter. The integrated curvature $\mathscr{K}$ has been the subject of some studies in the nuclear context, where it appears that the coefficient c_3 may be close to zero [18, 29]. It might thus turn out that in order to discuss the average nuclear energy to order A^0 the only new shape functional required beyond the surface energy $\mathscr{S}$ is the integrated squared curvature $\mathscr{Q}$.

Note that in the case of certain crevices the higher-order curvature corrections in the leptodermous expansion might diverge near or at the edge of the crevice. In such cases a more satisfactory overall energy expression would be obtained by *not* retaining these terms, at least not in the neighborhood of the crevice. Note also that for large overlaps the terminology of a "surface-layer energy" and a "proximity energy" should be modified. Thus for large overlaps this energy will be composed of an energy associated with the bulk of the overlap region, and of a surface-layer energy of a new kind, associated with the surface dividing the double-density and single-density regions. It is then more natural to make the obvious decomposition of this energy into new bulk and surface-layer terms, and not refer to it as a "proximity energy." (For a calculation of the new surface energy coefficient, see Ref. [16].)

Corrections to the gap or crevice energies given by Eq. (1) (arising, for example, from deviations from parallelism of the juxtaposed surface elements) have not been analyzed systematically. This should be done in order to clarify the range of applicability of the Proximity Formula. Some empirical information on this point is provided by the comparisons in Section 4.3.

Note that the implicit definition of γ through Eq. (16) depends on the choice of the surface Σ on which the surface elements $d\sigma$ are defined. Thus if one chose a different surface Σ' with whose surface elements $d\sigma'$ one were to label the "normal tubes," the resulting local surface energy γ' would be different, even though the product $d\sigma'\gamma'$ is, by definition, the same for a given tube. It follows that the total surface-layer energy E_{SL} is invariant with respect to a change from Σ to another reference surface Σ', but the local surface energy γ' is not, transforming in fact in a simple geometrical way as the reciprocal of the surface element $d\sigma'$ that intercepts a given tube. It follows that the *sum* of all the terms in Eq. (13) is invariant to changes from Σ to Σ', but the division into individual terms in the series is not. For example, if the surface Σ' is chosen to differ from the effective sharp surface by a small constant normal displacement (say of the order of the surface width b), then it is readily verified that even though the surface energy coefficients c_2 are the same in the two cases, the curvature correction coefficients c_3, c_4, etc., are different. It is, in fact, possible to pick a surface, say Σ_t, whose fixed normal displacement with respect to Σ is just such that the curvature correction coefficient c_3 vanishes identically. (Such a surface is sometimes referred to as the "surface of tension.") Another possibility would be to choose, instead of Σ, the half-density surface $\Sigma_{1/2}$ (the surface where the density has dropped to half its bulk value) or, perhaps, its generalization, the "central surface" Σ_c. (See the next section.) It then turns out that both c_2 and c_3 are the same for the two choices $\Sigma_{1/2}$ (or Σ_c) and Σ, but that the higher order coefficients are different.

Insofar as a diffuse density distribution has no unique surface, the fact that there is a certain amount of arbitrariness in the choice of a reference surface within the surface region is natural, and it need cause no difficulties if one is always careful to specify the surface with respect to which one has chosen to calculate the curvature correction coefficients c_3, c_4, etc. In making this choice one should bear in mind the following. The half-density surface $\Sigma_{1/2}$ or, preferably, the central surface Σ_c, are better suited for describing the location in space of the diffuse density profile. The surface of tension

Σ_t is better suited for describing the location in space of the surface-energy bump $\eta - a_B\rho$. The effective sharp surface Σ has the advantage that the volume $\mathscr{V}$ it encloses is related simply to the bulk density ρ_B and to the number of particles by $A = \rho_B\mathscr{V}$. For the other surfaces the relation involves, besides the volume enclosed, other properties of the surfaces, such as their areas or integrated curvatures. This has led in the past (and, we fear, will continue to lead in the future) to drastic misunderstandings in the identification of the correct value of even the surface energy coefficient c_2! This results from a mixing up of the true surface energy, associated with the surface region, with a contribution from the *bulk*, which arises when the bulk density is made (unwittingly) a function of the shape or size of the system by demanding that the volume inside some surface other than Σ be constant. (See Ref. [24] and Ref. [17, p. 19].) In view of the uniquely simple relation between the effective sharp surface and the bulk density and particle number, we tend to single out Σ as the standard reference surface, introducing other surfaces such as Σ_c only when there is a special reason to do it.

The confusion arising when the bulk density is *unwittingly* made a function of shape or size should be distinguished clearly from the discussion of real, physical effects associated with explicit variations of the bulk density of a system. Such variations may result from the seeking out by a system in equilibrium of the configuration of minimum potential energy. (For example, light nuclei tend to have higher equilibrium bulk densities than heavy nuclei because they are squeezed more strongly by the surface tension and dilated less strongly by the electrostatic repulsion.) Once the relevant dependences of the coefficients c_1, c_2, c_3, etc., on the bulk density are known (or an assumption is made about the functional form of these dependences) there is no difficulty (though there are subtleties) in setting up the equations that describe the variations of the equilibrium bulk densities with size and shape of the system. An example of this is provided by the Droplet Model (Refs. [18, 19]).

The Droplet Model also provides an illustration of the way deviations from a strictly leptodermous situation may be treated. Thus when the long-range electrostatic interaction is included in the idealized nuclear problem the bulk density is no longer constant, but exhibits instead a gentle variation. This variation may, however, be separated from the rapid density decrease in the surface, and the system may still be considered as leptodermous in an extended sense. The resulting energy expressions are derived in Refs. [18, 19].

3.1. Geometrical Properties

For the practical utility of the Proximity Theorem it turns out to be of the utmost importance to be precise in defining the relative positions of the diffuse surfaces of two interacting leptodermous systems. (The strong interaction between two such systems has a range of the order of the surface diffuseness and unless the surface positions are specified to within a fraction of this already small number the calculated interaction will be correspondingly in error.) In this connection we shall clarify some elementary geometrical properties of diffuse surfaces in a way that follows the much more exten-

sive works of Süssmann [20] and Myers [21] (which, however, were specialized to spherical shapes).

Consider a diffuse distribution in space defined by first choosing a uniform distribution bounded by the effective sharp surface Σ and by then moving matter from inside to outside this surface according to some falloff profile $f(n)$, a function of the normal distance from Σ. The function $f(n)$ is supposed to drop from one to zero in some (small) distance of order b, say, and to have an intrinsic shape independent of the position on Σ. As before construct normal tubes subtending elements of area $d\sigma$ on Σ. If the amount of matter in a tube after the diffusing of the surface is to be equal to the amount before we must have

$$d\sigma \int_{-N}^{\infty} dn(1 + \kappa n) f(n) = d\sigma \int_{-N}^{0} dn(1 + \kappa n). \tag{21}$$

Here $(1 + \kappa n) \, dn \, d\sigma$ is the volume element in the integration along a tube, the familiar factor $1 + \kappa n$ correcting for the slight nonuniformity in the tube cross section associated with the small curvature κ of the surface Σ (e.g., Ref. [17, p. 58]). The lower limit $-N$ is assumed to be sufficiently deep inside the distribution, where $f(-N)$ is essentially unity, so that Eq. (21) is essentially independent of N.

Integrating the left side of Eq. (21) by parts and the right directly and rearranging gives

$$\int_{-N}^{\infty} n(-(df/dn)) \, dn + \tfrac{1}{2}\kappa \int_{-N}^{\infty} n^2(-(df/dn)) \, dn$$

$$= N[1 - f(-N)] - \tfrac{1}{2}\kappa N^2[1 - f(-N)] \approx 0. \tag{22}$$

The negative of the derivative of the profile function, $(-df/dn)$, has the appearance of a bump in the surface region which, for a leptodermous system, is assumed to fall off rapidly away from the surface. The two terms on the left of Eq. (22) are thus proportional to the first and second moments of the bump function evaluated with respect to the origin of the normal coordinate n, which was taken to be on the surface Σ. (These moments are essentially independent of $-N$, which we shall put equal to $-\infty$.) Following Süssmann we shall define the "central surface" Σ_c to be located at such a value of n, denoted by n_c, that the first moment of the profile bump function taken with respect to n_c is zero. Thus

$$\int_{-\infty}^{\infty} (n - n_c)(-(df/dn)) \, dn = 0. \tag{23}$$

This "central surface" is thus at the *center* of gravity of the profile bump function (hence the name) and may be used to specify the *location* of the diffuse surface. In this respect it is analogous to the half-density surface but, being an integral quantity, does not suffer from the arbitrariness of being associated with a particular value of the

density (the half value). In order to solve explicitly for the distance n_c of the central surface from the effective sharp surface we write

$$n^2 = [(n - n_c) + n_c]^2$$
$$= (n - n_c)^2 + 2n_c(n - n_c) + n_c^2,$$

and substitute in Eq. (22), using Eq. (23):

$$(n_c + \tfrac{1}{2}\kappa n_c^2) \int_{-\infty}^{\infty} (-(df/dn))\, dn + \tfrac{1}{2}\kappa \int_{-\infty}^{\infty} (n - n_c)^2\, (-(df/dn))\, dn = 0.$$

It follows that, for $\kappa n_c \ll 1$,

$$n_c = -\tfrac{1}{2}\kappa b^2 + \cdots, \tag{24}$$

where

$$b = \left[\int_{-\infty}^{\infty} (n - n_c)^2\, (-(df/dn))\, dn \right]^{1/2}$$

is the r.m.s. width of the profile bump function, Süssmann's "width" of the diffuse surface.

Equation (24) is the generalization of Süssmann's relation for spherical systems between the effective sharp radius R and the central radius C (Ref. [21, p. 468]):

$$C = R(1 - (b^2/R^2) + \cdots),$$

that is,

$$C - R = (b^2/R) + \cdots.$$

Since for a sphere the curvature κ is $2/R$ Eqs. (24) and (25) agree.

The position of the surface of tension was derived on p. 58 of Ref. [17]. By writing the surface-layer energy including the curvature correction as

$$E_{SL} = \int_{\Sigma} d\sigma\, (\gamma_0 + (\partial\gamma/\partial\kappa)_{\text{plane}}\, \kappa + \cdots)$$
$$= \int_{\Sigma} d\sigma\, (1 + l\kappa)\, \gamma_0,$$

where $l = (1/\gamma_0)(\partial\gamma/\partial\kappa)_{\text{plane}}$, one realizes that the surface-layer energy is, to the relevant approximation, an integral of the *standard* surface energy γ_0 but over a surface shifted normally by the length l (which is equal to the ratio c_3/c_2 of the curvature and surface energy coefficients in Eq. (20)). This shift to the "surface of tension," displaced by a constant from the effective sharp surface Σ, may thus be used to absorb the curvature correction in the surface energy.

3.2. Comments

We hope to have clarified somewhat the content of leptodermous energy formulas of the type of Eqs. (13), (14). Formulas like this are often thought of in the context

of a Liquid Drop Model of nuclei, which historically has tended to be identified with systems of strongly interacting particles characterized by short mean-free-paths, and treated according to classical mechanics. As a result formulas of the type of Eqs. (13), (14), with their bulk and surface-layer energies have been thought to be in conflict with the independent-particle model of nuclei, which is characterized by particles with long mean-free-paths, treated quantally. Our derivation of the leptodermous energy formula shows, we hope, that classical assumptions about the treatment of the constituents of the system do not enter, and that no assumptions about the mean-free-paths are necessary. The crucial assumption on which the leptodermous energy formula is based is the relative thinness of the surface layer, and this need not be in conflict with a model of quantized independent (long mean-free-path) particles.

In fact, Refs. [17, 19, 22, 23, 24, 25] illustrate precisely how in the case of either independent or interacting particles treated quantally the energy density function $\eta - a_B \rho$ remains confined to the vicinity of the surface and the leptodermous condition is satisfied. Thus if the Thomas–Fermi approximation is used to treat the problem of quantized interacti nucleons [19] the deviations of the densities and energy densities from their bulk values tend to disappear exponentially as one leaves the surface region along the inward normal. (The disappearance is even more rapid towards the outside.) In the case of a Hartree treatment of a semi-infinite system, where a product wave function is used, the energy density function $\eta - a_B \rho$ is also confined to the surface region [23] (although the tail extending inward exhibits oscillations and must be treated with care). The use of a determinantal wave function [22] does not appear to change things appreciably. For a finite system (e.g., completely independent quantized particles in a box) the oscillations in the densities may be appreciable, especially for boxes possessing a high degree of symmetry. This is associated with shell effects (due to the discreteness of the particles, augmented by degeneracies associated with symmetries). The problem of isolating in that case the smooth, shell-averaged, background in the energy expressions is a subtle one and has been the subject of many recent investigations. However, studies of special cases, such as those in Refs. [24, 25] illustrate how even then a leptodermous expansion is able to represent accurately the average of the total energy (a sum over energy eigenvalues).

Since one also knows experimentally that most nuclei are relatively thin-skinned systems, one may, we feel, use the leptodermous formula for nuclear energies without undue reservations on the score that one is "just parametrizing" nuclear masses in an ad hoc way. The essential reservation to keep in mind is that the formula refers to smooth, shell-averaged trends of the nuclear energy.

4. APPLICATIONS TO NUCLEI

4.1. The Universal Functions

It is convenient to introduce the following dimensionless proximity function

$$\phi(\zeta) = e(\zeta b)/2\gamma,$$

obtained from $e(s)$ by measuring the separation s in units of the surface width b, $\zeta = s/b$, and by measuring energy in units of twice the surface energy coefficient γ (the γ_0 of the previous section).

Similarly we define the dimensionless (incomplete) proximity moments by

$$\Phi_n(\zeta) = \int_\zeta^\infty \zeta^n \phi(\zeta) \, d\zeta = \mathscr{E}_n(\zeta b)/2\gamma b^{n+1}.$$

(For the zeroth moment Φ_0 we shall simply write Φ.)

By dealing with these dimensionless functions one can make the predictions of the theory insensitive to certain quantitative shortcomings of the models of the nuclear surface that have to be used in calculating $e(D)$ and its integrals. Thus a model of the surface could be somewhat inaccurate in reproducing the *absolute values* of the experimental surface energy and/or width (diffuseness) and, nevertheless, generate relatively accurate dimensionless functions ϕ and Φ. Combining these functions as predicted by the model with the *experimental* values of γ and b (rather than with the possibly inaccurate values given by the model) will then result in the most reliable exploitation of the theory, where the model of the surface only enters in determining the *functional form* (but not the scale) of the proximity functions.

We have carried out a calculation of the universal nuclear proximity function ϕ and of the associated moment functions Φ_n using the nuclear Thomas–Fermi model with Seyler–Blanchard phenomenological nucleon–nucleon interactions (Refs. [19, 23, 26]). Appendix A gives a brief description of the model and its adaptation to the calculation of the proximity energy. The resulting function $\phi(\zeta)$ is displayed in Fig. 2 and the integrated function $\Phi(\zeta)$ in Fig. 3. Table I gives $\phi(\zeta)$ together with its first four incomplete moments $\Phi(\zeta)$, $\Phi_1(\zeta)$, $\Phi_2(\zeta)$, and $\Phi_3(\zeta)$.

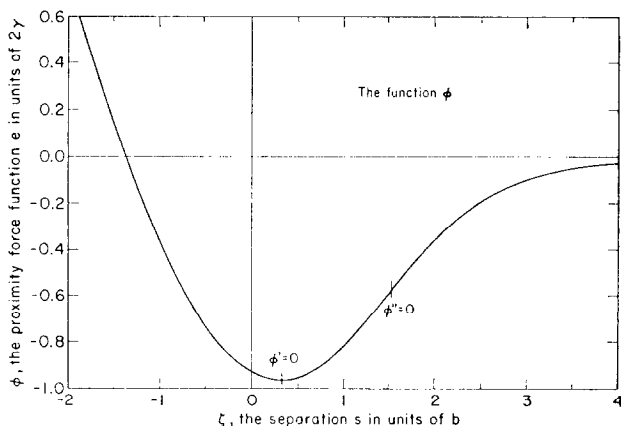For practical applications it is useful to have available a simple analytical represen-

FIG. 2.   The dimensionless proximity force function $\phi(\zeta)$ as a function of the dimensionless separation ζ. The minimum and point of inflexion in ϕ are indicated.
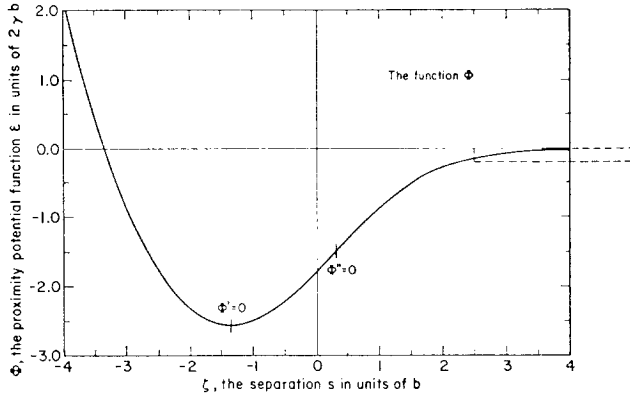
FIG. 3. The dimensionless proximity potential function $\Phi(\zeta)$ as a function of the dimensionless separation ζ. The minimum (at $\zeta = -1.3734$) and the point of inflexion in Φ are indicated. The potential between two nuclei is a geometrical factor times Φ. It follows that the equilibrium point (in the separation degree of freedom) for the nuclear interaction between any two nuclei occurs at the universal interpenetration distance of 1.3734 b or about 1.37 fm. The dashed rectangle on the right indicates the region where a comparison of the function Φ is made with experimental values in Fig. 9, using an expanded scale.

tation of the function Φ which enters in the nucleus–nucleus proximity potential that follows from Eq. (6)

$$V_P = 4\pi\gamma\bar{R}b \cdot \Phi(\zeta). \tag{26}$$

One such approximation is given by the following "cubic-exponential" pocket formula [27]:

$$\Phi(\zeta \leqslant \zeta_1) = -\tfrac{1}{2}(\zeta - \zeta_0)^2 - k(\zeta - \zeta_0)^3,$$
$$\Phi(\zeta \geqslant \zeta_1) = -3.437 \exp(-\zeta/0.75), \tag{27}$$

where $\zeta_1 = 1.2511 \approx 5/4$, $\zeta_0 = 2.54$, and $k = 0.0852 \approx 1/12$. This pocket formula for Φ is illustrated (by the circles) in Fig. 4, and should be adequate for many purposes. The cubic expression has been chosen to go smoothly to zero and so it could be used by itself in cases where the tail of the interaction is not an important feature. Approximate expressions for the higher moments Φ_n can be obtained by integrating Eq. (27). One can also obtain an approximation to ϕ by differentiating Eq. (27), but the result is only a rough representation, since a discontinuity in the slope of ϕ appears at $\zeta = 1.2511$ (a result of the discontinuity in the curvature in Eq. (27) at that point).

4.2. Suggested Parameters

In applications of the above formulas to nuclear problems the following choice of numerical parameters would be reasonable.

BŁOCKI ET AL.

TABLE I

ζ	ϕ	Φ	Φ_1	Φ_2	Φ_3
−3.50	3.0459	0.4697	−10.1755	20.811	−82.44
−3.45	2.9632	0.3195	−9.6534	18.997	−76.13
−3.40	2.8808	0.1734	−9.1530	17.283	−70.26
−3.35	2.7987	0.0314	−8.6738	15.665	−64.80
−3.30	2.7169	−0.1064	−8.2153	14.141	−59.73
−3.25	2.6355	−0.2403	−7.7771	12.705	−55.03
−3.20	2.5545	−0.3700	−7.3586	11.356	−50.68
3.15	2.4738	−0.4957	−6.9595	10.088	−46.65
−3.10	2.3935	−0.6174	−6.5792	8.900	−42.94
−3.05	2.3136	−0.7351	−6.2173	7.787	−39.52
−3.00	2.2342	−0.8488	−5.8734	6.747	−36.37
−2.95	2.1551	−0.9585	−5.5469	5.775	−33.48
−2.90	2.0766	−1.0643	−5.2375	4.870	−30.83
−2.85	1.9984	−1.1661	−4.9446	4.028	−28.41
−2.80	1.9208	−1.2641	−4.6678	3.246	−26.20
−2.75	1.8437	−1.3582	−4.4066	2.521	−24.19
−2.70	1.7671	−1.4485	−4.1606	1.851	−22.36
−2.65	1.6910	−1.5350	−3.9293	1.232	−20.71
−2.60	1.6155	−1.6176	−3.7123	0.662	−19.21
−2.55	1.5406	−1.6965	−3.5092	0.139	−17.86
−2.50	1.4662	−1.7717	−3.3193	−0.339	−16.65
−2.45	1.3925	−1.8432	−3.1424	−0.777	−15.57
−2.40	1.3194	−1.9109	−2.9780	−1.176	−14.60
−2.35	1.2470	−1.9751	−2.8256	−1.538	−13.74
−2.30	1.1753	−2.0357	−2.6848	−1.865	−12.98
−2.25	1.1042	−2.0926	−2.5552	−2.160	−12.31
−2.20	1.0339	−2.1461	−2.4362	−2.425	−11.72
−2.15	0.9644	−2.1960	−2.3276	−2.661	−11.21
−2.10	0.8956	−2.2425	−2.2288	−2.871	−10.76
−2.05	0.8276	−2.2856	−2.1394	−3.057	−10.37
−2.00	0.7604	−2.3253	−2.0590	−3.220	−10.04
−1.95	0.6941	−2.3617	−1.9871	−3.362	−9.76
−1.90	0.6287	−2.3947	−1.9235	−3.484	−9.53
−1.85	0.5642	−2.4246	−1.8676	−3.589	−9.33
−1.80	0.5006	−2.4512	−1.8190	−3.678	−9.17
−1.75	0.4379	−2.4746	−1.7773	−3.752	−9.04
−1.70	0.3763	−2.4950	−1.7422	−3.812	−8.93
−1.65	0.3156	−2.5123	−1.7132	−3.861	−8.85
−1.60	0.2560	−2.5266	−1.6900	−3.899	−8.79
−1.55	0.1975	−2.5379	−1.6721	−3.927	−8.75

TABLE I (*Continued*)

ζ	ϕ	Φ	Φ_1	Φ_2	Φ_3
−1.50	0.1401	−2.5463	−1.6592	−3.947	−8.72
1.45	0.0838	−2.5519	−1.6510	−3.959	−8.70
1.40	0.0287	−2.5547	−1.6470	−3.965	−8.69
−1.35	−0.0252	−2.5548	−1.6468	−3.965	−8.69
−1.30	−0.0779	−2.5522	−1.6503	−3.960	−8.70
−1.25	−0.1294	−2.5471	−1.6569	−3.952	−8.71
−1.20	−0.1795	−2.5393	−1.6663	−3.940	−8.72
−1.15	−0.2284	−2.5291	−1.6783	−3.926	−8.74
−1.10	−0.2759	−2.5165	−1.6925	−3.910	−8.75
−1.05	−0.3220	−2.5016	−1.7085	−3.893	−8.77
−1.00	−0.3667	−2.4843	−1.7262	−3.875	−8.79
−0.95	−0.4100	−2.4649	−1.7451	−3.856	−8.81
−0.90	−0.4519	−2.4434	−1.7650	−3.838	−8.83
−0.85	−0.4922	−2.4197	−1.7857	−3.820	−8.84
−0.80	−0.5310	−2.3942	−1.8068	−3.803	−8.86
−0.75	−0.5683	−2.3667	−1.8281	−3.786	−8.87
−0.70	−0.6040	−2.3374	−1.8493	−3.771	−8.88
−0.65	−0.6381	−2.3063	−1.8703	−3.757	−8.89
−0.60	−0.6706	−2.2736	−1.8907	−3.744	−8.90
−0.55	−0.7014	−2.2393	−1.9104	−3.732	−8.91
−0.50	−0.7306	−2.2035	−1.9292	−3.723	−8.91
−0.45	−0.7581	−2.1662	−1.9469	−3.714	−8.91
−0.40	−0.7838	−2.1277	−1.9633	−3.707	−8.92
−0.35	−0.8079	−2.0879	−1.9782	−3.702	−8.92
−0.30	−0.8302	−2.0469	−1.9915	−3.697	−8.92
−0.25	−0.8508	−2.0049	−2.0031	−3.694	−8.92
−0.20	−0.8696	−1.9619	−2.0128	−3.692	−8.92
−0.15	−0.8866	−1.9180	−2.0204	−3.691	−8.92
−0.10	−0.9018	−1.8732	−2.0260	−3.690	−8.92
−0.05	−0.9153	−1.8278	−2.0294	−3.690	−8.92
0.00	−0.9270	−1.7817	−2.0306	−3.690	−8.92
0.05	−0.9369	−1.7351	−2.0294	−3.689	−8.92
0.10	−0.9450	−1.6881	−2.0259	−3.689	−8.92
0.15	−0.9514	−1.6407	−2.0199	−3.688	−8.92
0.20	−0.9560	−1.5930	−2.0116	−3.687	−8.92
0.25	−0.9589	−1.5451	−2.0008	−3.685	−8.92
0.30	−0.9601	−1.4971	−1.9876	−3.681	−8.92
0.35	−0.9595	−1.4491	−1.9720	−3.676	−8.92
0.40	−0.9573	−1.4012	−1.9541	−3.669	−8.92
0.45	−0.9535	−1.3534	−1.9338	−3.660	−8.91

BLOCKI ET AL.

TABLE I (*Continued*)

ζ	ϕ	Φ	Φ_1	Φ_2	Φ_3
0.50	−0.9480	−1.3059	−1.9112	−3.650	−8.91
0.55	−0.9410	−1.2586	−1.8864	−3.637	−8.90
0.60	−0.9325	−1.2118	−1.8594	−3.621	−8.89
0.65	−0.9225	−1.1654	−1.8305	−3.603	−8.88
0.70	−0.9111	−1.1196	−1.7995	−3.582	−8.87
0.75	−0.8983	−1.0743	−1.7667	−3.558	−8.85
0.80	−0.8842	−1.0297	−1.7322	−3.532	−8.83
0.85	−0.8689	−0.9859	−1.6960	−3.502	−8.80
0.90	−0.8524	−0.9429	−1.6584	−3.469	−8.78
0.95	−0.8348	−0.9007	−1.6194	−3.433	−8.74
1.00	−0.8161	−0.8594	−1.5791	−3.393	−8.70
1.05	−0.7965	−0.8191	−1.5378	−3.351	−8.66
1.10	−0.7761	−0.7798	−1.4955	−3.306	−8.61
1.15	−0.7549	−0.7415	−1.4525	−3.257	−8.56
1.20	−0.7329	−0.7043	−1.4088	−3.206	−8.50
1.25	−0.7104	−0.6682	−1.3646	−3.152	−8.43
1.30	−0.6873	−0.6333	−1.3200	−3.095	−8.36
1.35	−0.6638	−0.5995	−1.2753	−3.036	−8.28
1.40	−0.6400	−0.5669	−1.2304	−2.974	−8.19
1.45	−0.6159	−0.5355	−1.1857	−2.910	−8.10
1.50	−0.5917	−0.5053	−1.1412	−2.845	−8.01
1.55	−0.5674	−0.4763	−1.0970	−2.777	−7.90
1.60	−0.5431	−0.4486	−1.0533	−2.708	−7.80
1.65	−0.5190	−0.4220	−1.0101	−2.638	−7.68
1.70	−0.4950	−0.3967	−0.9677	−2.567	−7.56
1.75	−0.4713	−0.3725	−0.9260	−2.495	−7.44
1.80	−0.4480	−0.3495	−0.8852	−2.423	−7.31
1.85	−0.4250	−0.3277	−0.8454	−2.350	−7.18
1.90	−0.4026	−0.3070	−0.8066	−2.277	−7.04
1.95	−0.3807	−0.2874	−0.7689	−2.205	−6.90
2.00	−0.3595	−0.2689	−0.7324	−2.133	−6.76
2.05	−0.3389	−0.2515	−0.6970	−2.061	−6.61
2.10	−0.3190	−0.2350	−0.6629	−1.990	−6.47
2.15	−0.2998	−0.2196	−0.6301	−1.921	−6.32
2.20	−0.2815	−0.2050	−0.5985	−1.852	−6.17
2.25	−0.2639	−0.1914	−0.5681	−1.784	−6.02
2.30	−0.2471	−0.1786	−0.5391	−1.718	−5.87
2.35	−0.2312	−0.1667	−0.5113	−1.654	−5.72
2.40	−0.2162	−0.1555	−0.4847	−1.591	−5.57
2.45	−0.2019	−0.1450	−0.4594	−1.529	−5.42

TABLE I (*Continued*)

ζ	ϕ	Φ	Φ_1	Φ_2	Φ_3
2.50	−0.1885	−0.1353	−0.4353	−1.469	−5.27
2.55	−0.1759	−0.1262	−0.4123	−1.411	−5.12
2.60	−0.1641	−0.1177	−0.3904	−1.355	−4.98
2.65	−0.1531	−0.1098	−0.3696	−1.300	−4.84
2.70	−0.1427	−0.1024	−0.3498	−1.248	−4.70
2.75[a]	−0.1331	−0.0955	−0.3310	−1.196	−4.56
2.80	−0.1242	−0.0890	−0.3132	−1.147	−4.42
2.85	−0.1158	−0.0831	−0.2963	−1.099	−4.28
2.90	−0.1080	−0.0775	−0.2802	−1.053	−4.15
2.95	−0.1007	−0.0722	−0.2649	−1.008	−4.02
3.00	−0.0939	−0.0674	−0.2504	−0.965	−3.89
3.05	−0.0876	−0.0628	−0.2367	−0.924	−3.77
3.10	−0.0817	−0.0586	−0.2237	−0.884	−3.64
3.15	−0.0762	−0.0547	−0.2114	−0.845	−3.52
3.20	−0.0711	−0.0510	−0.1997	−0.808	−3.40
3.25	−0.0663	−0.0475	−0.1886	−0.772	−3.29
3.30	−0.0618	−0.0443	−0.1781	−0.738	−3.18
3.35	−0.0577	−0.0414	−0.1682	−0.705	−3.07
3.40	−0.0538	−0.0386	−0.1588	−0.673	−2.96
3.45	−0.0502	−0.0360	−0.1499	−0.643	−2.86
3.50	−0.0468	−0.0336	−0.1415	−0.614	−2.75

[a] For $\zeta > 2.74$ the functions $\phi(\zeta)$ and $\Phi(\zeta)$ are exact exponentials with a range 0.7176 (equal to the Yukawa range 0.62567 fm of the Seyler–Blanchard interaction, measured in units of the Thomas–Fermi surface width of 0.872 fm, see Appendix A).

For the surface energy coefficient γ one might use the Lysekil mass formula of Ref. [28] according to which

$$\gamma = 0.9517[1 - 1.7826 I^2] \text{ Mev/fm}^2, \qquad (28)$$

where $I = (N - Z)/A$, and N, Z, and A refer to the combined system of the two interacting nuclei. In this way some allowance is made for the dependence of the proximity potential on the neutron excess, even though the universal functions ϕ and Φ were calculated for zero neutron excess. (A rough approximation to γ would be simply $(1 - 2I^2)$ MeV/fm^2.)

In calculating the value of $\bar{R}$ in Eq. (26) and the separation $s = r - C_1 - C_2$ for spherical nuclei the surfaces should be located using Süssmann's central radius C, related to the effective sharp radius by Eq. (25). (In the case of more general geometries
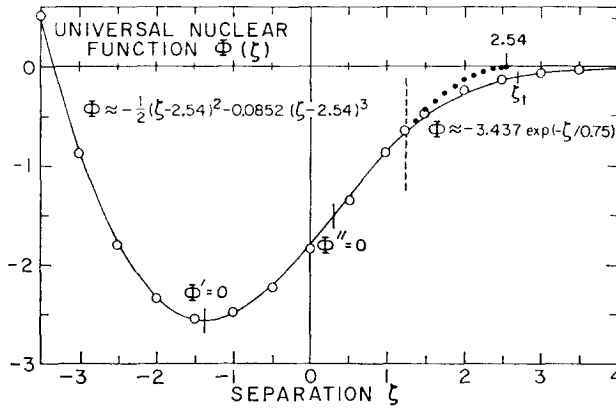
FIG. 4. The universal nuclear function Φ is shown by the solid line and the cubic-exponential approximation by circles. The dots show the continuation of the cubic beyond the dashed line (locating its junction with the exponential) to where it touches the ζ-axis at 2.54. The frozen Thomas–Fermi densities of the two semi-infinite distributions touch at $\zeta_t = 2.74$.

the central surface Σ_c should be used, related to the effective sharp surface Σ by Eq. (24).) For the effective sharp radius one may use the formula

$$R = 1.28A^{1/3} - 0.76 + 0.8A^{-1/3} \tag{29}$$

$$\approx 1.15A^{1/3}\text{fm}. \tag{30}$$

When used in conjunction with the Proximity Force Theorem the central radius is preferable to the effective sharp radius R, which moves *out* relative to the density profile by an amount proportional to $A^{-1/3}$ (Eq. 25), and which is not, therefore, in an invariant relation to the location of the profile for finite nuclei with different radii. Note that the Proximity Force Theorem is based on Eq. (1), whose physical content is the approximate replacement of the interaction energy of two curved surfaces by an integral of the interaction energy per unit area of parallel flat surfaces for which the separation $D(x, y)$ matches, point by point, the distance between pairs of elements of the actual curved surfaces. In order for the approximation to be accurate the flat surfaces should be located so that their profiles match the *locations* of the actual profiles as well as possible. This is ensured to a higher degree of accuracy by working with the central radius C rather than with the effective sharp radius R. (See below.)

Nevertheless, we consider R as the primary quantity for which we provide empirical expressions (Eqs. (29), (30)) because it is R and not C which is exactly proportional to $A^{1/3}$ for incompressible systems, and nearly proportional to $A^{1/3}$ for nearly incompressible systems such as nuclei. A refined analysis of the experimental evidence on nuclear sizes indicates [21, 29] that $R/A^{1/3}$ is to a fair approximation constant at about 1.15 fm. A slight variation from about 1.11 fm for $A \approx 20$ to 1.18 for $A \approx 250$ is the expected result of the finite compressibility of nuclei, leading to a relatively greater squeezing of light nuclei by the surface-tension forces and the dilation of heavy nuclei by the electrostatic repulsion. An attempt to take this into account is

represented by Eq. (29). This value of R, when divided by $A^{1/3}$, reproduces closely the middle curve in Fig. 5 of Ref. [29], representing average nuclear matter radii between $A = 20$ and $A = 250$. It is important to stress that neither the coefficient 1.28 of $A^{1/3}$ in Eq. (29) nor the 1.15 in Eq. (30) is to be interpreted as the nuclear radius constant of nuclear matter, whose value, as deduced in Ref. [29], is 1.18 fm $\pm$ about 0.02 fm.
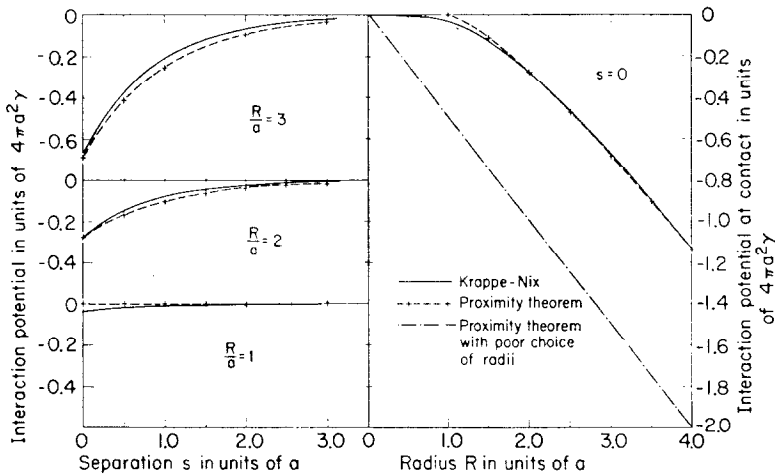

FIG. 5. A comparison of the exact interaction between two equal Krappe–Nix spheres (solid lines) and the approximation resulting from applying the Proximity Theorem to properly chosen effective spheres (dashed lines and crosses). The dot-dashed line corresponds to a poor choice of the radii of the interacting objects.

The width b in Eq. (26) has the approximate value of 1 fm. Thus for a Woods–Saxon surface profile the Süssmann width b is related to the "10–90 fall-off distance" by [Ref. 21]

$$b = [\pi/(2(3)^{1/2} \ln 9)] \, t_{10-90} \, ,$$

which for $t_{10-90} = 2.4$ fm gives 0.99 fm. For a more refined analysis of the course of the neutron, proton and average surface widths throughout the periodic table see Ref. [11]. As a nominal value of b we shall, however, use 1 fm.

The above equations give only average estimates of nuclear sizes. Variations caused by shell effects, including deformations, have to be taken into account separately. In particular, when using the proximity potential for deformed nuclei, the distance of closest approach s, as well as the mean curvature radius $\bar{R}$ of the gap width function in the vicinity of the point of closest approach, have to be carefully related to the orientations and shapes of the nuclei.

In the formulas given above there are no adjustable parameters in the predicted nucleus–nucleus interaction. For some purposes it might be useful to have adjustable parameters that could be varied, within reasonable limits, in correlating experimental data. For example, some slight variations in the nuclear radii from the nominal values

given by Eqs. (29), (30) would be reasonable. Similarly the nominal values of the surface energy coefficient γ (Eq. (28)) and of the surface width b (= 1 fm) need not, of course, remain inviolate. Altogether the slight freedoms associated with adjustments in the values of the radius, surface energy, and surface width are together equivalent to slight freedoms representing a horizontal shift, and horizontal and vertical stretchings of the nucleus–nucleus potential $V_P(r)$. Such adjustments of the parameters should, however, be used with moderation and should not be in conflict with what is known about nuclear radii and surface properties. In particular, if in the interpretation of nucleus–nucleus scattering experiments by means of the frozen idealization (in which all degrees of freedom except the separation between nuclei are frozen), unreasonable adjustments of the parameters are called for, the explanation is very likely to be the inadequacy of the frozen idealization. One would then be wiser to display clearly the discrepancies rather than to mask the *expected* failure of the frozen idealization by an abuse of the nuclear parameters.

With reference to some earlier misunderstandings, let us stress that the use of the proximity energy expressions (as generalized in Section 2.2 for various geometrical arrangements including necks and crevices) is not tied to the frozen idealization. Thus if a neck degree of freedom is added in the description of (e.g., deep inelastic) scattering, an appropriate proximity energy formula, taken for example from Section 2.2, may be used.

4.3. *Tests of the Leptodermous Formula*

The accuracy of the leptodermous energy expressions (13), (14) depends on the smallness of the ratio b/R_0. How accurate should one expect the expressions to be in nuclear applications where this ratio may not be very small, especially for light nuclei?

We shall first test Eqs. (13), (14) against the exactly soluble mathematical model of Krappe and Nix [4] of two sharp spheres (with surface separation s), whose volume elements interact by a Yukawa interaction of range a and strength written as $V_0/4\pi a^3$. For a single such sphere of radius R the exact energy is

$$V = V_0[-4\pi R^3/3 + 2\pi a R^2 + O \cdot a^2 R - 2\pi a^3 + 2\pi a(R + a)^2 \exp(-2R/a)].$$

With $V_0 = 2.2105$ MeV/fm^3, $a = 1$ fm, $R = 1.2\, A^{1/3}$ fm (values representative of the nuclear situation) this gives (in MeV)

$$V = -16A + 20A^{2/3} + O \cdot A^{1/3} - 13.89 + 13.89(1.2A^{1/3} + 1)^2 \exp(-2.4A^{1/3})$$
$$= -250 + 125 + 0 - 13.89 + 0.55, \quad \text{for} \quad A = 15.625 \text{ (i.e., } A^{1/3} = 2.5).$$

Equations (13), (14) applied to this case give

$$V = 2.2105 \text{ (MeV/fm}^3)[\mathscr{V} + \tfrac{1}{2}a\mathscr{S} + O \cdot \mathscr{K} - \tfrac{1}{8}a^3\mathscr{G} - (3/32)\, a^3\mathscr{D}]$$
$$= 2.2105 \text{ (MeV/fm}^3)[-4\pi R^3/3 + 2\pi a R^2 + 0 - 2\pi a^3]$$
$$= -250 + 125 + 0 - 13.89 \text{ MeV}.$$

(In Ref. [27, p. 5] the coefficients of $\mathscr{G}$ and $\mathscr{D}$ were interchanged.)

In this case the only term not reproduced by the leptodermous formula is the exponential one, amounting to 0.55 MeV. This may not be a representative figure, however, because in the Krappe–Nix model the polynomial part of the energy expression happens to terminate at the A^0 term. If this is a peculiarity of the model then in a more general case one might expect the next term to be of order $(10\text{--}20)\, A^{-1/3}$ MeV, i.e., a few million electron volts rather than $\frac{1}{2}$ MeV for $A \approx 16$, somewhat less for larger systems.

For two equal Krappe–Nix spheres, whose centers are separated by r, the exact additional interaction energy may be written as

$$
\begin{aligned}
V_{\text{int}}/4\pi a^2 \gamma &= -4(\rho \cosh \rho - \sinh \rho)^2 \, (r/a)^{-1} \exp(-r/a) \\
&= -4(\rho \cosh \rho - \sinh \rho)^2 \, (\sigma + 2\rho)^{-1} \exp(-\sigma - 2\rho),
\end{aligned}
\tag{31}
$$

where $\rho = R/a$, $\sigma = s/a$, and γ, equal to $aV_0/2$, is the surface energy coefficient in the Krappe–Nix model. (In Ref. [27, p. 5] there is a misprint in the formula for V_{int}.)

In the example under consideration the value of V_{int} is -9.35 MeV for $\sigma = 0$, and -2.95 MeV for $\sigma = 1$.

In applying the proximity formula (6) to this case we first note that the interaction energy per unit area between two Krappe–Nix slabs is readily verified to be

$$
e(s) = -2\gamma e^{-s/a}.
$$

In inserting this in Eq. (6) (where $\bar{R} = C_1 C_2/(C_1 + C_2)$) we shall use for the effective central radius C_{eff} of a Krappe–Nix object (a sharp sphere generating a diffuse potential) the mean between the central radii of the density and potential distributions

$$
C_{\text{eff}} = \tfrac{1}{2}(C_\rho + C_V),
$$

where

$$
\begin{aligned}
C_\rho &= R, \\
C_V &= R(1 - b^2/R^2 + \cdots).
\end{aligned}
$$

Here b is the Süssmann width of the surface of the diffuse potential distribution. In the Krappe–Nix case it is related simply to the range of the Yukawa interaction by $b = 2^{1/2}a$ (Ref. [21], Eq. (18)). Thus the effective radius of the interacting spheres is

$$
C_{\text{eff}} = R(1 - a^2/R^2 + \cdots),
$$

and the separation between their effective surfaces is

$$
s_{\text{eff}} = r - 2R(1 - a^2/R^2) = s + 2a^2/R.
$$

Inserting these values in the formula

$$V_P = -4\pi\gamma a \cdot \frac{C_{\text{eff}}^2}{C_{\text{eff}} + C_{\text{eff}}} \, e^{-s_{\text{eff}}/a},$$

we find

$$V_P/4\pi\gamma a^2 = -\tfrac{1}{2}(\rho - \rho^{-1}) \exp(\quad \sigma \quad 2\rho^{-1}). \tag{32}$$

(In [27, p. 6] there is a misprint in the exponent.) This formula gives -9.51 MeV for $\sigma = 0$ and -3.50 MeV for $\sigma = 1$ as the interaction energy in the case under considera-tion, when $R = 3$ fm and $a = 1$ fm, so that $\rho = 3$.

The upper left-hand part of Fig. 5 compares the exact interaction energy (Eq. (31)) with the proximity formula (Eq. (32)) for $R/a = 3$. The other two graphs make the comparison for $R/a = 2$ and 1.

On the right the exact and approximate interaction energies at contact ($s = 0$) are compared as functions of R/a. Also shown (by the dot–dash curve) is the result of not being careful in the choice of the effective location of the surface of a Krappe–Nix object. This curve is the result of taking R instead of C_{eff} to locate the surface. This leads to

$$V_P = -4\pi\gamma a \cdot \frac{R^2}{R + R} \cdot e^{-(r-2R)/a},$$

or

$$V_P/4\pi\gamma a^2 = -\tfrac{1}{2}\rho \exp(-\sigma).$$

This expression, even though formally correct in the limit of very large ρ, would be useless in practice for ρ-values in the range around 2–5.

These comparisons illustrate the importance of recognizing the proper location of the surface profiles of the curved objects to which the Proximity Theorem is being applied. This has to do with the importance of properly matching the parallel flat surfaces (underlying the Proximity Theorem) to the profiles of the curved surface elements that the flat surfaces are supposed to represent. In the Krappe–Nix case this proper matching makes all the difference between the theorem being a useless curiosity and a practical tool for predicting the results of a calculation, without carrying out the somewhat involved multiple integrations associated with folding in (Yukawa) interactions. We should remark, however, that the Krappe–Nix case, with a *sharp* density but a *diffuse* potential, is a situation that exaggerates this aspect of the problem. It is only because the density is sharp that its profile stays at R whereas the location of the potential profile moves in by b^2/R as the surface is curved. In a self-cohesive system (such as a nucleus), where the density generates the potential and the potential determines the density in a self-consistent way, the widths of the potential and density profiles are approximately equal, and the density and potential profiles do not move appreciably with respect to each other as the surface is curved. Applying the Proximity Theorem simply to the matter density radii C_ρ (as was implicitly suggested in Section 4.2) should then be a fairly adequate procedure.

The Proximity Theorem was tested also for the case of unequal Krappe–Nix spheres, with similar results to those described above. In addition, in Ref. [30], an exhaustive series of comparisons was made for a generalized Krappe–Nix model where equal or unequal *diffuse* spherical density distributions were used to generate diffuse potentials by way of Yukawa interactions of various ranges. A limiting case is that of two diffuse spherical distributions whose elements interact by zero-range (delta-function) forces. In all cases the proximity formula was a useful approximation, provided the effective surfaces of the interacting systems were properly located at the average position between the density and potential surface locations. In the most realistic cases where the density and potential had comparable diffuseness the agreement was even closer than in the extreme case of a sharp density, illustrated in Fig. 5.

A second comparison of the nuclear proximity potential was made, this time with the interaction potential between model nuclei described with the aid of a simplified Thomas–Fermi method (the energy–density formalism of Ref. [2]).

Figure 6 shows such a comparison for the case of ^{40}Ar $+$ ^{121}Sb and Fig. 7 for ^{84}Kr $+$ ^{209}Bi. The calculated potentials are generally similar, but one should bear in mind that in such comparisons one is not just testing the Proximity Theorem but also the correctness of some of the parameters used in the energy–density formalism. (In
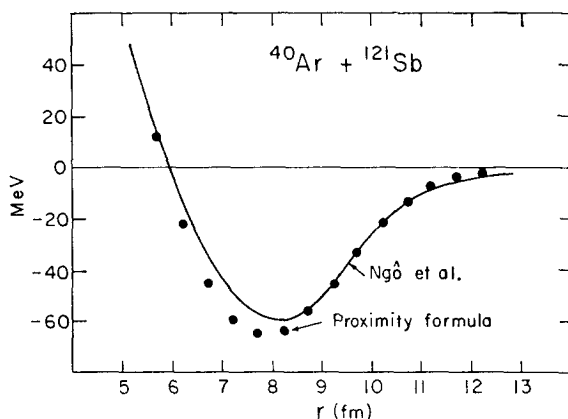
FIG. 6.   A comparison of the interaction potential between ^{40}Ar and ^{121}Sb calculated using the energy–density formalism (line) and the Proximity Theorem (dots). In constructing the proximity potentials in Figs. 6, 7, and 8 the radii were calculated according to $R = (1.13 + 0.0002A)A^{1/3}$ fm. This is an older version of Eq. (29). In the cases illustrated the difference between the two empirical expressions for R is negligible.

particular those combinations of parameters that control the values of the nuclear radii, surface energy and diffuseness.) Thus if a set of parameters is used in the energy–density formalism that does not reproduce experimental nuclear properties well, a relatively large deviation from the proximity potential (with its parameters taken from experiment) may be expected. This is illustrated in Fig. 8 based on Ref. [31]. Here the dashed line refers to a set of parameters (Set II) preferred by the authors, and the solid
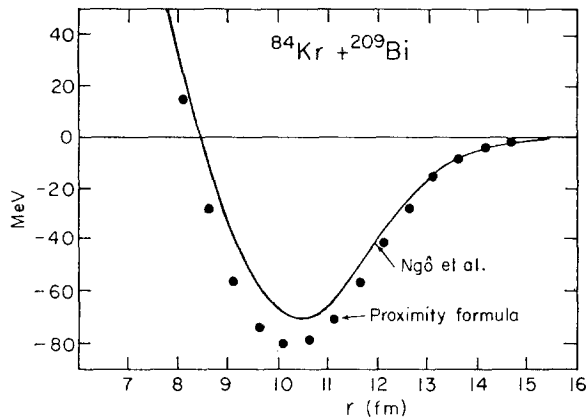
FIG. 7. Same as Fig. 6 but for [84]Kr and [209]Bi. The energy–density calculations are described in Ref. [3]; a more detailed table on which the present curves are based were supplied courtesy of Professor D. Sperber.
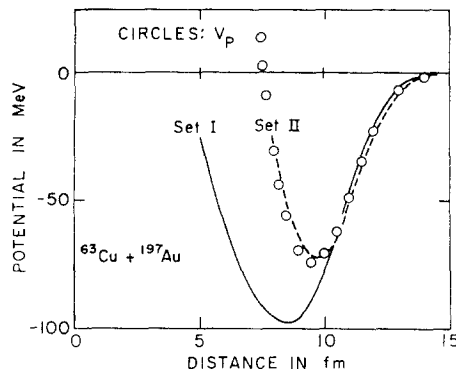

FIG. 8. The proximity potential V_P between [63]Cu and [197]Au (circles) is compared with the calculations of Ref. [31]. The dashed curve refers to a calculation with a favored set of parameters, the solid curve to an earlier version.

curve to an earlier set of parameters, which shows rather large deviations from the proximity potential.

As remarked by the authors of Ref. [31] their results are consistent with the Proximity Theorem in the sense that the interaction potentials for 17 pairs of nuclei (calculated with one and the same set of parameters) can be reduced approximately to a universal function of the separation between the nuclear surfaces by dividing out an estimated reduced radius, roughly proportional to $A_1^{1/3} A_2^{1/3}/(A_1^{1/3} + A_2^{1/3})$. To test quantitatively the accuracy of the Proximity Theorem in this way it would be necessary to determine the surface locations (central radii C_1 and C_2) of the model nuclei employed, and to use these values in making the reduction of the interaction curves to a universal function.

We have recently become aware of an analysis of elastic scattering data in Ref. [34] which makes possible a comprehensive comparison of the theoretical proximity potential with experiment in the extreme tail region (see Fig. 3). As discussed in Ref. [34], the results of 57 elastic scattering experiments (involving projectiles ranging from ^{10}B to ^{32}S and targets from ^{11}B to ^{208}Pb) can be used to deduce, for each pair of nuclei, a value of a potential depth V_{exp} at a certain distance r_{exp} between the centers of the interacting nuclei (a distance related to the rainbow angle). By dividing the potential by the factor $4\pi\gamma b\bar{R}$ appropriate to the system in question, an experimental value of Φ_{exp} may be deduced. The dimensionless separation ζ_{exp} at which this value is plotted as a point in Fig. 9 is obtained by subtracting from r_{exp} the appropriate sum of the central radii $C_{Target} + C_{Projectile}$ (obtained using Eqs. (29) and (25)) and dividing by b ($= 1$ fm).

Figure 9 shows that the theoretical value of the interaction function Φ in the
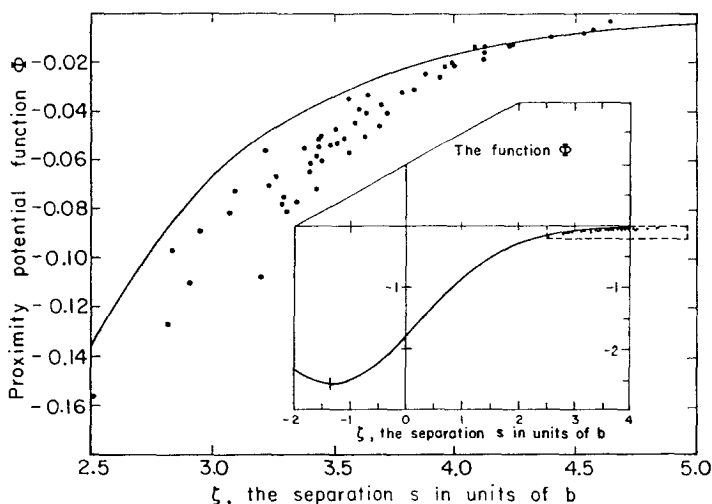
FIG. 9.   A comparison of the extreme tail of the universal function Φ (see Fig. 3) with experimental values deduced from an analysis of elastic scattering data (Ref. [34]). The inset on the right, with a few experimental points, serves to recall the original scale of the function Φ in Fig. 3.

extreme tail is of the order of magnitude of the experimental points and that it exhibits the observed trend with separation. To what extent the deviations are significant is not clear at the moment, the *systematic* deviation (most points lie to the right of the curve) could be removed by a 2 % increase in the nominal radius formula Eq. (29), used to deduce ζ_{exp} from r_{exp}. But there is no reason to think that this is necessarily the explanation of the deviations.

Based on these and other comparisons carried out so far, our impression is that the suggested simple scheme of estimating the nucleus–nucleus potential (in the separation degree of freedom), using for example the pocket formula (27) and experimental values of nuclear radii, surface energy, and diffuseness, should be useful down to quite

small systems, with A values perhaps below even $A = 16$. In the later stages of a nucleus–nucleus interaction, when a crevice or neck has formed, the appropriate proximity energy expression should also continue to be useful in correcting the grossest shortcomings of the polynomial part of the leptodermous expansion, Eq. (20). A study of this problem is under way.

As a final application of the proximity function ϕ we might mention the estimate of the tensile strength of (a cylinder of) nuclear matter against a disruption into two pieces with two new surfaces facing each other across a gap. (In nuclear fission the question sometimes arises as to the smallest neck that could withstand the electrostatic repulsion between the fragments before rupturing by way of such a new degree of freedom, not included in the usual parametrizations of fissioning shapes.)

If the rupture is assumed to proceed along a degree of freedom that is essentially the reverse of the bringing together of two juxtaposed surfaces with frozen density profiles, the force necessary to cause rupture is proportional to

$$-\frac{\partial e(s)}{\partial s}\bigg|_{max} = -\frac{2\gamma}{b}\frac{\partial}{\partial\zeta}\phi(\zeta)\bigg|_{max}.$$

Using Table I we find that the maximum value of ϕ' is about 0.486 (at $\zeta = 1.55$). With the nominal values of γ and b we then find for the tensile strength the simple result of just about (1 MeV/fm) per fm².

In conclusion we hope that this paper will be useful in advancing our quantitative understanding of macroscopic nuclear properties and that, perhaps, it might also be found to have relevance in the domain of surface physics.

Appendix A

In this Appendix we give a brief outline of the adaptation of the Seyler–Blanchard nuclear model to the calculation of the proximity functions.

The model is based on the following phenomenological nucleon–nucleon interaction [26]

$$V_{12} = -C\,\frac{e^{-r_{12}/a}}{r_{12}/a}\,(1 - p_{12}^2/b^2).$$

Here r_{12} is the separation between the two nucleons and p_{12} their relative momentum. The parameters entering are: a, the range of the Yukawa interaction, b, the critical momentum at which the interaction turns repulsive, and C ($=C_l$ or C_u), the interaction strength, which is different for like and unlike nucleon pairs. For symmetric systems (identical neutron and proton distributions) only the average strength $C = \frac{1}{2}(C_l + C_u)$ enters.

The associated nuclear many-body problem is treated in the Thomas–Fermi approximation. In this approximation the local Fermi momentum $P_F(\mathbf{r})$ determines the matter density $\rho(\mathbf{r})$ ($\sim P_F(\mathbf{r})^3$) as well as the kinetic-energy density $\tau(\mathbf{r})$ ($\sim P_F(\mathbf{r})^5$). Because of the quadratic momentum dependence, the energy density in the presence of the Seyler–Blanchard interaction can be expressed solely in terms of the distributions

ρ and τ. Moreover, since $\tau \sim \rho^{5/3}$, it follows that the energy of the system is determined once the matter density distribution ρ has been specified. The various relevant formulas can be found in Ref. [23].

The fact that the energy density is uniquely determined once the matter density ρ has been specified is exploited in the calculation of the proximity energy. The matter density distribution associated with the combined system is simply the superposition of the two individual density distributions, each of which is given as the equilibrium distribution associated with one isolated semi-infinite system.

The actual calculation of the function ϕ displayed in Fig. 2 is performed as follows. First, the problem of one isolated symmetric semi-infinite system is solved as in Ref. [23]. This determines the density profile of the standard nuclear surface, and in particular its energy and diffuseness. The parameter values employed are those determined in Ref. [19]. They are

$$a = 0.62567 \text{ fm,}$$

$$b = 392.48 \text{ MeV/c,}$$

$$C = 328.61 \text{ MeV.}$$

This leads to a surface energy of $\gamma_{\text{TF}} = 1.017$ MeV/fm^2 and a surface diffuseness of $b_{\text{TF}} = 0.872$ fm when a radius constant r_0 equal to 1.2049 fm is used, see Ref. [19]. As remarked in Section 4.1 the fact that these numbers may not be the most accurate representations of the experimental values of γ and b is largely immaterial for the calculation of ϕ and Φ.

Subsequently, two identical semi-infinite systems are positioned with a certain separation s between the locations of their parallel surfaces. The two density profiles are assumed to remain frozen in their asymptotic, isolated form. Then the total matter density is obtained by superposition and the total energy, relative to the energy of two infinitely separated systems, is calculated (per unit surface area). The universal dimensionless proximity function $\phi(\zeta)$ is obtained by measuring the calculated energy per unit area in units of twice the surface energy $\gamma_{1\text{F}}$ and the surface separation s in units of the diffuseness b_{TF}.

REFERENCES

1. W. GREINER, Proceedings of Heavy-Ion Summer Study at Oak Ridge National Laboratory, p. 1. June 12–July 1, 1972.
2. K. A. BRUECKNER, J. R. BUCHLER, S. JORNA, AND R. J. LOMBARD, *Phys. Rev.* **171** (1968), 1188.
3. For example, C. NGÔ *et al., Nucl. Phys. A* **240** (1975), 353; J. GALIN *et al., Phys. Rev. C* **9** (1974), 1018.
4. H. J. KRAPPE AND J. R. NIX, Proceedings of the Third IAEA Symposium on Physics and Chemistry of Fission, Rochester, New York, p. 159, August 1973.
5. D. M. BRINK AND N. ROWLEY, *Nucl. Phys. A* **219** (1974), 79.
6. R. A. BROGLIA AND A. WINTHER, *Phys. Rep.* **4** (1972), 153.
7. J. WILCZYŃSKI, *Nucl. Phys. A* **216** (1973), 386.
8. R. BASS, *Phys. Lett. B* **47** (1973), 139.
9. B. DERYAGIN (DERJAGUIN), *Kolloid Z.* **69** (1934), 155; see also Ref. [33].
10. J. RANDRUP, Nuclear Chemistry Annual Report, Lawrence Berkeley Laboratory Report LBL-2366, p. 137, 1973.
11. W. D. MYERS AND H. VON GROOTE, Lawrence Berkeley Laboratory Report LBL-4327, October 1975, submitted to *Phys. Lett. B*.
12. J. N. ISRAELACHVILI AND D. TABOR, *Proc. Roy. Soc. Ser. A* **331** (1972), 19.
13. K. L. JOHNSON, K. KENDALL, AND A. O. ROBERTS, *Proc. Roy Soc. Ser. A* **324** (1971), 301.
14. T. D. LEE AND G. C. WICK, *Phys. Rev. D* **9** (1974), 2291.
15. W. BARDEEN *et al., Phys. Rev. D* **11** (1975), 1094; A. CHODOS *et al., Phys. Rev. D* **9** (1974), 3471.
16. J. RANDRUP, to be published.
17. W. D. MYERS AND W. J. SWIATECKI, *Nucl. Phys.* **81** (1966), 1.
18. W. D. MYERS AND W. J. SWIATECKI, *Ann. Physics* **84** (1974), 186.
19. W. D. MYERS AND W. J. SWIATECKI, *Ann. Physics* **55** (1969), 395.
20. G. SÜSSMANN, Lawrence Berkeley Laboratory Report LBL-1615 (1973).
21. W. D. MYERS, *Nucl. Phys. A* **204** (1973), 465.
22. W. J. SWIATECKI, *Proc. Phys. Soc. London Sect. A* **64** (1951), 226.
23. J. RANDRUP, Lawrence Berkeley Laboratory Report LBL-4302 (1975); *Nucl. Phys. A* **259** (1976), 253.
24. C. F. TSANG, Ph.D. Thesis, University of California Radiation Laboratory Report UCRL-18899 (May 1969).
25. W. J. SWIATECKI, "Nuclear Reactions Induced by Heavy Ions" (R. Bock and W. R. Herring, Eds.), p. 729, North–Holland, Amsterdam, 1970. W. D. MYERS, *in* "Dynamic Structure of Nuclear States," Proceedings of the 1971 Mont Tremblant International Summer School, University of Toronto Press, 1972.
26. R. G. SEYLER AND C. H. BLANCHARD, *Phys. Rev.* **124** (1961), 227; **131** (1963), 355.
27. W. J. SWIATECKI, "Macroscopic Description of the Interaction Between Two Complex Nuclei," Lecture presented at the International School Seminar on Reactions of Heavy Ions with Nuclei and Synthesis of New Elements, Dubna, USSR, September 23–October 4, 1975; Lawrence Berkeley Laboratory Report LBL-4296, September 1975.
28. W. D. MYERS AND W. J. SWIATECKI, *Ark. Fys.* **36** (1967), 343.
29. W. D. MYERS, Lawrence Berkeley Laboratory Report LBL-4332 (October 1975), to appear in Atomic Data and Nuclear Data Tables, 1976.
30. J. RANDRUP, Lawrence Berkeley Laboratory Report LBL-4317 (1975).
31. C. NGÔ *et al., Nucl. Phys. A* **252** (1975), 237.
32. H. S. M. COXETER, "Introduction to Geometry," Wiley, New York/London, 1961.
33. B. DERYAGIN *et al., J. Colloid. Interface Sci.* **53** (1975), 314.
34. P. R. CHRISTENSEN AND A. WINTHER, *Phys. Lett.*, to be published.